The yeast telomerase RNA, TLC1, participates in two distinct modes of TLC1-TLC1 association processes *in vivo*

Elizabeth Blackburn, Tet Matsuguchi

Telomerase core enzyme minimally consists of the telomerase reverse transcriptase domain-containing protein (Est2 in budding yeast *S. cerevisiae*) and telomerase RNA, which contains the template specifying the telomeric repeat sequence synthesized. Here we report that *in vivo*, a fraction of *S. cerevisiae* telomerase RNA (TLC1) molecules form complexes containing at least two molecules of TLC1, via two separable modes: one requiring a sequence in the 3’ region of the immature TLC1 precursor and the other requiring Ku and Sir4. Such physical TLC1-TLC1 association peaked in G1 phase and did not require telomere silencing, telomere tethering to the nuclear periphery, telomerase holoenzyme assembly, or detectable Est2-Est2 protein association. These data indicate that TLC1-TLC1 associations reflect processes occurring during telomerase biogenesis; we propose that TLC1-TLC1 associations and subsequent reorganization may be regulatory steps in telomerase enzymatic activation.

The Yeast Telomerase RNA, TLC1, Participates in Two Distinct Modes of TLC1-TLC1 Association Processes *in vivo*

ABSTRACT

Telomerase core enzyme minimally consists of the telomerase reverse transcriptase domain-containing protein (Est2 in budding yeast *S. cerevisiae*) and telomerase RNA, which contains the template specifying the telomeric repeat sequence synthesized. Here we report that *in vivo*, a fraction of *S. cerevisiae* telomerase RNA (TLC1) molecules form complexes containing at least two molecules of TLC1, via two separable modes: one requiring a sequence in the 3' region of the immature TLC1 precursor and the other requiring Ku and Sir4. Such physical TLC1-TLC1 association peaked in G1 phase and did not require telomere silencing, telomere tethering to the nuclear periphery, telomerase holoenzyme assembly, or detectable Est2-Est2 protein association. These data indicate that TLC1-TLC1 associations reflect processes occurring during telomerase biogenesis; we propose that TLC1-TLC1 associations and subsequent reorganization may be regulatory steps in telomerase enzymatic activation.

AUTHORS

Tet Matsuguchi

Elizabeth H. Blackburn

Department of Biophysics and Biochemistry

University of California, San Francisco

San Francisco, CA

United States of America

Corresponding Author

Elizabeth H. Blackburn

600 16th Street Box 2200

San Francisco, CA 94158-2517

415-476-2824

Elizabeth.Blackburn@ucsf.edu

INTRODUCTION

Telomeric DNA is typically composed of repetitive sequences (TG1-3 repeats in the budding yeast *S. cerevisiae*) that allow recruitment of specialized macromolecular complexes that help replenish and protect telomeres (de Lange, Lundblad & Blackburn, 2006). These include the ribonucleoprotein telomerase, which adds telomeric DNA by the action of its reverse transcriptase-containing subunit (Est2 in *S. cerevisiae*), templated by a sequence within the telomerase RNA component (TLC1 in *S. cerevisiae*), as well as telomere-protective double-stranded and single-stranded telomeric DNA binding proteins, such as Rap1 and Cdc13 in yeast (Jain & Cooper, 2010).

Budding yeast telomerase RNA, TLC1, is over 1300 nucleotides in size and, in addition to providing the template for reverse transcription, has extensive secondary structures (Zappulla & Cech, 2004). Certain structures within TLC1 have been defined and form binding sites for Est2 and other telomerase factors. The critical central core of TLC1 includes a structurally highly conserved pseudoknot to which Est2 binds, while an Sm-protein binding site is located near the 3' end, which is important for the stability and processing of immature TLC1 (Seto et al., 2002; Zappulla & Cech, 2004; Lin et al., 2004; Jiang et al., 2013) (Figure 1A). Previously, it was reported that mutations (*tlc1-42G* and *tlc1-42C*) in a 6-base palindromic sequence, located within the TLC1 precursor 3' region that is cleaved off to form the processed mature TLC1 RNA (see Figure 1A), cause telomeres to be shorter *in vivo* and abrogate dimerization of TLC1 precursor synthesized *in vitro* (Gipson et al., 2007). Additionally, a 48-nucleotide stem motif in TLC1 directly binds the Ku70/Ku80 complex, which, in addition to its widely conserved canonical role in non-homologous end joining (NHEJ), is required for many aspects of yeast telomere biology (Stellwagen et al., 2003). This TLC1-Ku interaction, while not absolutely required for telomere maintenance by telomerase *in vivo*, is required for maintenance of full-length telomeres, *in vivo* association of Est2 to telomeres in G1 phase of the cell cycle (Fisher, Taggart & Zakian, 2004), full recruitment of telomeres to the nuclear periphery (Taddei et al., 2004), and transcriptional silencing at telomeres (Boulton & Jackson, 1998). A mutant Ku containing a small insertion, *yku80-135i*, specifically abrogates the TLC1-Ku interaction but leaves NHEJ intact (Stellwagen et al., 2003). Est1 and Est3 are essential factors for telomerase, which together with Est2 and

TLC1, make up the telomerase holoenzyme. Est1 associates with the telomerase complex by directly binding to a bulge-stem region of TLC1 conserved in several budding yeasts, and this association is critical for the recruitment of telomerase to telomeres (Seto et al., 2002; Chan, Boulé & Zakian, 2008).

Human, *S. cerevisiae*, and *Tetrahymena* (ciliated protozoan) telomerases have been inferred to be active as a monomer *in vitro* (Bryan, Goodrich & Cech, 2003; Alves et al., 2008; Shcherbakova et al., 2009; Jiang et al., 2013). However, reports have also suggested that the human, *S. cerevisiae*, and *Euplotes* (ciliated protozoan) telomerase complexes can exist in a dimeric (or other oligomeric) forms (Prescott & Blackburn, 1997; Wenz et al., 2001; Beattie et al., 2001; Wang, Dean & Shippen, 2002). Recent single-molecule electron microscopic structural determinations indicate that core human telomerase complex (telomerase RNA, hTER, and reverse transcriptase, hTERT) is a dimer *in vitro* held together by RNA-RNA (hTER-hTER) interaction (Sauerwald et al., 2013).

Here, we explored possible modes of physical telomerase dimerization *in vivo,* focusing on the yeast telomerase RNA component TLC1. We developed a biochemical method that directly demonstrates a physical TLC1-TLC1 association (dimerization/oligomerization; direct or indirect), quantified in extracts of cells expressing normal amounts of telomerase RNA from the endogenous *TLC1* gene chromosomal locus. We have not determined whether there are more than two molecules of TLC1 that are associated in complexes, so for simplicity, we refer to this as TLC1-TLC1 association. We report here that such TLC1-TLC1 associations occur *in vivo* via two modes, each mode having distinctive requirements. Our evidence supports association between telomerase RNAs occurring during the biogenesis of active telomerase complex, with potential functional importance in the regulation of telomerase activity.

MATERIALS AND METHODS

Plasmids

The integrating vector, pRS306-TLC1, was provided by Jue Lin. The MS2 CP-binding RNA hairpins were constructed by annealing overlapping oligonucleotide in a standard PCR protocol.

The hairpin construct was cloned into the BclI site of pRS306-TLC1. The fusion PCR method was used to construct *tlc1-42G* and *tlc1-42C* alleles, which were cloned between the BclI and XhoI sites of pRS306-TLC1. CEN-ARS versions of the plasmids were made by subcloning BamHI-XhoI fragments of the integrating vectors into the vector pRS316.

Yeast strains and growth media

Yeast strains were in the S288c background and are isogenic with BY4746, except as noted in Table 1 (Baker Brachmann *et al.* 1998). Yeast cultures were grown in standard rich medium or minimal media (YEPD or CSM). Deletion strains were made using a PCR-based transformation method (Longtine *et al.* 1998).

Immunoprecipitation of MS2 hairpin-tagged TLC1

TLC1 was tagged with two MS2 coat-protein-binding RNA hairpins at the BclI restriction site in the *TLC1* coding region sequence. This gene construct with its native promoter was integrated at the endogenous chromosomal *TLC1* locus, in tandem with untagged, wild-type *TLC1*, flanking the *URA3* marker. MS2 coat protein fused to 3 Myc epitope tags was expressed either in *tlc1Δ* or in experimental strains containing both tagged and untagged *TLC1*. Whole cell lysates were prepared from cultures in log-phase of growth in YEPD (OD_{600}=0.6-1.0) using glass beads and bead beaters. The lysis buffer contained 50mM HEPES-KCl pH8.0, 2 mM EDTA, 2 mM EGTA, 0.1% Nonidet P40, 10% glycerol, cOmplete EDTA-free protease inhibitors (Roche) and RNasin (Promega; 1 uL / mL). The lysate concentrations were adjusted to A_{260nm} = 40 before immunoprecipitation. For lysates containing co-expressed MS2 coat protein, 400 uL of lysate was mixed with 1.5 mg Dynal ProA magnetic beads (Invitrogen) and 1 ug of monoclonal anti-Myc antibody (9E11, Santa Cruz Biotechnology). For experiments in which MS2 coat protein was purified separately, ProA magnetic beads, anti-Myc antibody, and whole cell lysate containing MS2 coat protein (at A_{260nm}=60-80) were incubated for 1-2 hours. The beads were washed and used for tagged TLC1 precipitation. The immunoprecipitation was allowed to take place at 4 °C for 4-hours to overnight. For oligonucleotide-directed displacement experiments, the immunoprecipitates were washed in presence of oligonucleotides each at 0.5 uM in the lysis buffer.

125 Immunoprecipitation of tagged proteins
126 For immunoprecipitation of tagged proteins (Est2-13xMyc, Est2-3xFLAG), lysates were
127 prepared as described above. For Myc-tagged proteins, the lysate was mixed with 1.5 mg Dynal
128 ProA magnetic beads, and 1 ug 9E11 antibody. For FLAG-tagged proteins, lysate was incubated
129 with 50uL of M2-conjugated agarose beads. For sequential immunoprecipitation of FLAG-
130 tagged proteins followed by Myc-tagged proteins, 15 ug of 3xFLAG peptide was added to the
131 M2-conjugated agarose beads. The eluate was then used for Myc-tag immunoprecipitation as
132 described.
133
134 Quantitative reverse transcription and PCR
135 RNA from input and immunoprecipitates were isolated using RNeasy Mini Kit (Qiagen),
136 including the DNase step as described by the manufacturer. The primer set for PGK1 was
137 designed using IDT's PrimerQuest program. The reverse primers used to distinguish tagged and
138 untagged TLC1 were designed within and at the insertion junction, respectively, of the MS2
139 hairpin tag. One-step reverse transcription and PCR kits were used for all RNA quantifications,
140 except for the quantification of immature TLC1 (Stratagene, Invitrogen). For quantification of
141 immature TLC1, or 3' regions of TLC1, SuperScript III and random hexamer were used for
142 reverse transcription. Subsequently, SYBR Green I Master mix kit (Roche) was used for
143 quantitative PCR. All quantitative PCR runs included serially diluted RNA samples to make
144 standard curve, from which relative quantitative values were derived using the LightCycler
145 software. The oligonucleotide sequences used in qRT-PCR reactions are listed in Table 2.
146
147 Telomere length analysis
148 Genomic DNA was digested with XhoI and separated on a 0.85% agarose gel. DNA was
149 denatured and transferred to a Nylon membrane, and UV-crosslinked with a Stratalinker. The
150 membrane was blotted with telomeric oligonucleotide
151 (5'-CACACCCACACCACACCCACAC-3') labeled with WellRED D3 fluorescent dye at the 5'
152 end. The blotted membrane was scanned and analyzed using the Odyssey Infrared Imaging
153 System (LI-COR). A linear plasmid containing an S. cerevisiae telomeric DNA sequence was
154 included as a marker.
155

156

157 RESULTS

158 Co-immunoprecipitation assays demonstrate TLC1-TLC1 association *in vivo*

159

160 To quantify the association between different TLC1 molecules in yeast whole-cell extracts, a co-
161 immunoprecipitation (coIP) assay was developed. First, we created a tagged TLC1 RNA for
162 immunoprecipitation using a tandem pair of RNA hairpins that specifically bind to the
163 bacteriophage MS2 Coat Protein. This two-hairpin construct was inserted at a site in a region of
164 TLC1 previously shown to accommodate insertions of modular protein binding domains with
165 minimal if any effect on *in vivo* functions (Bernardi & Spahr, 1972; Zappulla & Cech, 2004)
166 (Figure 1A). Secondly, we fused three copies of myc tag to MS2 Coat Protein and integrated this
167 gene construct into the genome of experimental strains. Co-expression of the MS2 hairpin-
168 tagged TLC1 (TLC1-MS2) and myc-tagged Coat Protein (CP-3myc) allowed specific
169 immunoprecipitation of TLC1-MS2 using an anti-myc antibody. Thirdly, we developed
170 quantitative RT-PCR assays to measure levels and recovery of TLC1, using two sets of PCR
171 primers capable of distinguishing and specifically amplifying either the untagged TLC1 or
172 TLC1-MS2 (Figure 1C).
173 Next, we verified that the insertion of the MS2 tag did not significantly alter TLC1 functions *in*
174 *vivo*. The expression level of TLC1-MS2 was comparable to untagged TLC1 (Figure 1D). The
175 association of TLC1-MS2 with Est2 was slightly reduced compared to untagged TLC1, and this
176 was further evidenced by slightly shorter but stable telomere lengths in cells expressing only
177 TLC1-MS2 (Figure 1E-F).

178

179 Finally, we co-expressed TLC1-MS2 and untagged TLC1 from the endogenous TLC1 locus to
180 test the coIP of untagged TLC1 with TLC1-MS2. As a control, an equal number of cells from
181 two independently cultured strains expressing either only untagged TLC1 or only TLC1-MS2
182 were mixed prior to cell lysis ("Mix" samples in figures). We found that 50-80% of total TLC1-
183 MS2 is immunoprecipitated from lysates made from the co-expression strain and from the mixed
184 population. A significant enrichment of untagged TLC1 in the TLC1-MS2 immunoprecipitate
185 was observed only in the co-expression strain and not in the mixed cell population, indicating
186 that this assay detected bona fide *in vivo* association of separate TLC1 molecules (see Materials

and Methods and Figure 1G). After adjusting for the immunoprecipitation efficiency and the fact that this coIP assay only detects heterodimer of TLC1-MS2 and untagged TLC1, we determined that in unsynchronized log phase cell populations, at least 10% of TLC1 is associated with another TLC1 *in vivo* (Figure 1G; see Materials and Methods for calculation). Interestingly, we observed that the fraction of immature TLC1 molecules present in the whole lysate (4-8%) (Mozdy & Cech, 2006) did not significantly change in the immunoprecipitate, indicating that both immature and mature forms of TLC1 participate comparably in TLC1-TLC1 association (Figure 1H).

The 3' Region of TLC1 is Important for TLC1-TLC1 association

To determine the regions of TLC1 involved in the TLC1-TLC1 physical association, we designed a nucleic acid competition experiment aimed to disrupt this association by incubating the TLC1 complex(es), extracted as the immunoprecipitates from cell lysates, with excess anti-sense oligonucleotides. We designed 72 overlapping DNA oligonucleotides, each 30 bases in length, that in total were complementary to the full length of the immature TLC1, which includes the 3' region that is cleaved off in the mature form (Figure 1B). These oligonucleotides were incubated with the TLC1-MS2 immunoprecipitate bound to the magnetic beads in the wash buffer (see Materials and Methods). We predicted that the collection of these 72 TLC1 antisense oligos would act as competitors to TLC1-TLC1 association in the immunoprecipitates. As a control, 72 different DNA oligonucleotides designed against other regions of the yeast genome were used. Incubation of the full set of 72 TLC1-antisense oligonucleotides (but not the 72 control oligonucleotides) with the immunoprecipitates reduced the amount of untagged TLC1 remaining on the affinity beads by about 70%, while not appreciably diminishing the amount of TLC1-MS2 remaining bound to the affinity beads (Figure 2A and B, bottom row). This result indicated that the 72 TLC1-antisense oligonucleotides likely disrupted the association of the untagged TLC1 and TLC1-MS2.

To further delineate the regions important for the TLC1-TLC1 association, different subsets of oligonucleotides were used in the same experimental set-up. The 72 oligonucleotides were subdivided into intervals encompassing thirds or ninths of the length of the immature TLC1, in

order to probe each TLC1 region separately (Figure 2B). The oligonucleotides complementary to the first third (the 5' region) of TLC1 had little effect on disrupting TLC1-TLC1 association, while the oligonucleotides against the central and 3' region intervals had greater effects (Figure 2B, Row 2). Even added together, the total of the effects from each of the three separate regions was significantly less than the disruptive effect seen when all 72 oligonucleotides were added simultaneously, suggesting that there is a synergistic effect in adding all oligonucleotides at once. Similarly, separately challenging the TLC1-TLC1 immunoprecipitates in this way with the anti-sense oligonucleotides encompassing each of the one-ninth regions, especially in the 5' regions of TLC1, disrupted the TLC1-TLC1 association to even lesser extents (Figure 2B Row 1).

Interestingly, TLC1-TLC1 association was disrupted by 30% using the eight antisense oligonucleotides encompassing the TLC1 3' region. Only two of these eight oligonucleotides were complementary to the last 21 bases of the mature form of TLC1; the remaining six oligonucleotides were complementary only to the 3' extension of the un-cleaved, immature form of TLC1 (Figure 1B). As described above, the immature TLC1 molecules accounted for only 4-8% of the total TLC1 signal in the immunoprecipitate (Figure 1H); thus, a reduction solely of immature TLC1 precursors cannot account for the 30% disruption by the 3' most one-ninth TLC1-complementary oligonucleotides. This result suggests that a small region (30 bases) encompassed by just two oligonucleotides had a relatively large effect in disrupting TLC1-TLC1 association of the mature form of TLC1.

Together, these findings indicated that the 3' region of TLC1 transcript is either the most critical for TLC1-TLC1 association to occur *in vivo*, and/or the most vulnerable to subsequent *in vitro* disruption of the associated form. This *in vitro* disruption by the 3' region-targeting oligonucleotides could have been through a direct competition of base-paired regions between two *TLC1* RNAs, through an unwinding of some structural elements of TLC1, or disruption of RNA-protein associations. Additionally, these data suggest that the TLC1-TLC1 association mostly involves tail-tail (*i.e.*, 3'region with 3' region) interactions, rather than head-head (*i.e.*, 5'region with 5' region) or head-tail (*i.e.*, 5'region with 3' region) formations.

Prompted by the importance of the 3' region of TLC1, we tested the potential role in TLC1-TLC1 association for a previously identified, palindromic sequence located in the 3' region cleaved off during TLC1 maturation and thus present only in the immature, precursor TLC1 molecules. This palindromic sequence is evolutionarily conserved among budding yeast species (Gipson et al., 2007). Two palindrome disruption mutations (*tlc1-42G* and *tlc1-42C*) that prevent potential intermolecular base-pairing by this sequence, and the compensatory mutations (*tlc1-42GC*), which restore the potential for intermolecular base-pairing but not the wild-type palindromic sequence itself, have been described previously (Gipson et al., 2007). We found that the palindrome disruption mutations *tlc1-42G* and *tlc1-42C*, when incorporated into untagged TLC1 in the strains also expressing TLC1-MS2, reduced TLC1-TLC1 coIP by over half (Figure 2C). The compensatory mutation, *tlc1-42GC*, although restoring intermolecular base-pairing potential, failed to restore the TLC1-TLC1 coIP level (Figure 2C). The total levels of these mutant telomerase RNAs were unchanged from wild type; hence, efficient *in vivo* association between mature TLC1 molecules requires the specific sequence - and not simply its potential for base pairing *in trans* - of a palindromic motif located in the cleaved-off 3' portion of the TLC1 precursor. These results indicate that at least some TLC1-TLC1 association initiates during telomerase biogenesis before processing produces the mature TLC1 3' end.

TLC1-TLC1 Association is dependent on nuclear export and is cell cycle-regulated

Maturation of telomerase RNA including 3' end processing takes place partially in the cytoplasm (Gallardo et al., 2008). Interestingly, while deletion of Tgs1, which is responsible for TLC1 m3G cap formation (Franke, Gehlen & Ehrenhofer-Murray, 2008), had no effect on total TLC1 levels and little effect on TLC1-TLC1 association ($p > 0.05$), mutating Nup133 (required for nuclear export) (Gallardo et al., 2008) diminished by at least half the fraction of TLC1 in the associated form, while causing no effect on total TLC1 levels ($p < 0.05$; Figure 3A). This finding indicated that TLC1 export into the cytoplasm may be necessary for TLC1-TLC1 association.

TLC1 maturation by 3' end processing is reported to be active only during G1 phase of the cell cycle (Chapon, Cech & Zaug, 1997). To test whether TLC1-TLC1 association is controlled during the cell cycle, yeast cell lysates were prepared at 15-minute intervals from cells following release into G1 phase from an alpha-factor arrest. Cell cycle progression and synchrony were

confirmed by analysis of the various cyclin mRNA levels throughout the time course (Figure 3B). Consistent with a previous report (Mozdy & Cech, 2006), the total TLC1 steady-state levels showed a slight increase as the cell cycle progressed (Figure 3C). During the first cell cycle after the release from the 2-hour alpha-factor arrest, the fraction of TLC1 in dimer form in the coIP assay remained relatively constant (Figure 3D). Then after mitosis, as the cell population re-entered the next G1 phase, the fraction of TLC1-TLC1 association abruptly increased 2-fold, with markedly different kinetics compared to the slow and steady accumulation of total TLC1throughout the cell cycle progression (Figure 3D). This finding is consistent with TLC1-TLC1 association occurring during the biogenesis of telomerase complex, a process that has been detected only in G1 phase. The lack of a higher fraction of TLC1 in the dimer form during the G1 phase immediately following the release from the 2-hour alpha-factor arrest is also consistent with TLC1-TLC1 association during a biogenesis step, since in this situation, cells have been held in G1 phase, in the presence of active biogenesis machinery, for 120 minutes prior to the point of release from alpha-factor. We conclude that TLC1-TLC1 association is cell-cycle-controlled and highest in G1.

Telomerase holoenzyme formation is not required for TLC1-TLC1 association

To test whether there are any protein factors that assist in maintaining the TLC1-TLC1 association, we treated the immunoprecipitates with trypsin. We found that protease treatment reduced coIP efficiency by ~40% compared with the control (Figure 4A; see Materials and Methods), suggesting a role for protein(s) in initiating, or stabilizing, TLC1-TLC1 association.

We tested the most likely protein factor candidate, Est2, the telomerase reverse transcriptase core protein. It has been shown that Est2 and TLC1 come together in the cytoplasm, although when in the cell cycle they initiate the interaction is unclear (Teixeira et al., 2002; Gallardo et al., 2008). In *est2Δ* strains, a diminution in TLC1-TLC1 association of about 20 – 25 % was detected, although this measured reduction was not highly significant when compared to the control wild-type *EST2* strain ($p > 0.05$; Figure 4B). We reasoned that the modest requirement for Est2 in TLC1-TLC1 association might be reflected in TLC1 mutants known to disrupt the core pseudoknot structure required for Est2-TLC1 interaction. Therefore, we disrupted the TLC1

pseudoknot by mutating either side of one stem (intra-base-pairing) made up of conserved sequences CS3 and CS4 (*tlc1-20* and *tlc1-21*), and restored the pseudoknot structure by the compensatory mutations (*tlc1-22*) (Lin et al., 2004). CoIP assays showed that the *in vivo* TLC1-TLC1 association was substantially reduced by the pseudoknot-disruptive mutations *tlc1-20* and *tlc1-21* and fully restored by the compensatory mutations, *tlc1-22* (Figure 4C). Thus, efficient TLC1-TLC1 association requires at least this aspect of normal folding of TLC1, although binding to Est2 is largely dispensable.

Next, we tested two other essential components of the telomerase holoenzyme, Est1 and Est3, for any roles in the *in vivo* TLC1-TLC1 association. Est1-TLC1 interaction is limited to S-phase of the cell cycle, and Est3 interaction with Est2 requires Est1 and hence is also S-phase dependent (Osterhage, Talley & Friedman, 2006). As in the *est2Δ* strain, the *est3Δ* strain showed a modest but not significant ($p > 0.05$) reduction in TLC1-TLC1 association. In *est1Δ*, however, the TLC1-TLC1 association was reduced by ~35% ($p < 0.05$). While many aspects of Est1 functions in telomere biology remain unclear, roles for Est1 in the recruitment of telomerase to telomeres as well as in telomerase enzymatic activation are well established (Evans & Lundblad, 2002). Thus TLC1-TLC1 association showed a somewhat greater dependence on Est1 than on Est2 and Est3. This raises the possibility that, rather than the telomerase enzymatic activation function of Est1, the telomere recruitment or other function unique to Est1 may play a role in TLC1-TLC1 association.

Ku and Sir4, but not Telomere Silencing or Tethering to the Nuclear Periphery, Promote the Same Mode of TLC1-TLC1 Association

To test whether other factors involved in telomerase recruitment to telomeres also affect TLC1-TLC1 association, we first performed the coIP assays in Ku mutant strains. In contrast to the more modest effects of the absence of essential telomerase components Est1, Est2 or Est3, 60 - 75% of the TLC1-TLC1 association was consistently lost in *yku70Δ* and *yku80Δ* strains, as well as in *yku80-135i* strains ($p < 0.00005$; Figure 4D), which have a small insertion in Ku that specifically abrogates TLC1-Ku interaction, but leaves NHEJ intact (Stellwagen et al., 2003). As previously reported (Mozdy, Podell & Cech, 2008), in all these Ku mutant strains the steady-

state level of total TLC1 was reduced by about 25-50% (Figure 4E), and telomeres, while stable, are shorter than in wild-type. Therefore we tested two different mutations (*cdc73Δ*, *ctr9Δ*) that reduce the steady-state level of TLC1 much more than the Ku mutations (Figure 4E). Neither *cdc73Δ* nor *ctr9Δ* caused any decrease in the fraction of dimeric TLC1 (Figure 4D). Furthermore, two mutations known to cause short telomeres (*arf1Δ and tel1Δ*) (Askree et al., 2004), also did not affect TLC1-TLC1 association (Figure 4D and E). The combined findings above indicate that Ku binding to TLC1 promotes or stabilizes TLC1-TLC1 association, and that neither reduction in TLC1 steady state level nor shorter, stable telomeres is sufficient to impair TLC1-TLC1 association.

The Ku complex is also necessary for telomere silencing (Boulton & Jackson, 1998) and telomere tethering to the nuclear periphery (Taddei et al., 2004). However, by using mutations that affect these processes, we found evidence that it is not because of these functions that Ku plays a role in TLC1-TLC1 association. Specifically, neither *sir2Δ* nor *sir3Δ* (which each abrogate telomere silencing) and neither *ctf18Δ* nor *esc1Δ* (which each diminish telomere tethering) (Hiraga, Robertson & Donaldson, 2006) decreased TLC1-TLC1 association levels (Figure 5A). In marked contrast, *sir4Δ* diminished TLC1-TLC1 association to the same extent as *yku80-135i* (Figure 5A). Sir4 is distinguished from the other telomere silencing Sir proteins Sir2 and Sir3 by its localization on telomeres closer to the distal tip than Sir2 and Sir3, and the Ku complex is reported to interact physically with Sir4 (Tsukamoto, Kato & Ikeda, 1997). Since Ku and Sir4 are localized on telomeres, we tested whether detection of TLC1-TLC1 association in cell extracts by the coIP assay was dependent on DNA. However, DNase treatment of the extracts did not diminish the fraction of TLC1 detected in dimeric form (Figure 5B and C).

To test if the Ku complex and Sir4 act in the same pathway for TLC1-TLC1 association, we combined *sir4Δ with yku80Δ* or *yku80-135i* mutations. The double mutants showed no further reduction in the TLC1 dimer fraction compared to single mutants (Figure 5C). We conclude that Ku binding to TLC1 and Sir4 regulates TLC1-TLC1 association through the same pathway, which is independent of telomere silencing or anchoring to the nuclear periphery.

Ku/Sir4 and the 3'-Cleaved TLC1 Precursor Sequence Promote TLC1-TLC1 association by Different Modes

To determine the relationship between the roles of Ku/Sir4 and the 3' region of TLC1 in TLC1-TLC1 association, we combined *sir4Δ* or *yku80Δ* mutation with the 3' mutation *tlc1-42G*. In these double mutants (*sir4Δ tlc1-42G* and *yku80Δ tlc1-42G* strains), compared to either each single-mutant strain or the *sir4Δ yku80Δ* double mutant, the TLC1-TLC1 association was further reduced, down to almost to the background control level (Figure 5D). This indicated that the TLC1-TLC1 association that is dependent on the 3' region of TLC1 is at least partially independent of Ku and Sir4, possibly mediated by a different pathway.

Lack of Evidence for Est2-Est2 Physical Association

Although, as described above, we did not find evidence that TLC1-TLC1 association was highly dependent on Est2, we tested the possibility that any of the small fraction of TLC1-TLC1 association that may be potentially affected by Est2 deletion might be mediated through association of one Est2 molecule with another Est2 molecule. To this end, we performed four different assays in attempts to detect any such physical Est2-Est2 interaction *in vivo*. First, we attempted to detect Est2-Est2 interaction by yeast two-hybrid assay in which Est2 was fused to the Gal4 activation domain and DNA binding domain separately; such assays showed no positive signals for Est2-Est2 interaction (data not shown). Secondly, we co-expressed Est2-FLAG and Est2-myc and performed co-immunoprecipitation assays; however, no signal indicative of co-immunoprecipitation was detected in the Western blots in these experiments (data not shown). Thirdly, to overcome the potential issues of the detection limit using Western blotting, we performed coIP experiments using presence of TLC1 as a proxy signal, via qRT-PCR assays as described above. In this approach, we co-expressed wild-type Est2-HA with either wild-type Est2-myc (positive control) or *est2ΔCP*-myc. *est2ΔCP* is a deleted Est2 that abrogates Est2-TLC1 interaction (Lin & Blackburn, 2004). Therefore, the presence of an interaction between Est2-HA and *Est2ΔCP*-myc can be ascertained by proxy using the measurement of TLC1 in *est2ΔCP*-myc IP. However, we did not observe any such enrichment of TLC1 in this coIP assay (Figure 6A). Finally, because TLC1 detection by the qRT-PCR assay had high sensitivity, we

also performed sequential coIP experiments with strains co-expressing Est2-FLAG and Est2-myc. In this assay, Est2-FLAG was adsorbed onto anti-FLAG gel matrix and subsequently eluted with FLAG peptide, and any Est2-myc present in the elution fraction was immunoprecipitated with anti-myc antibody. The amount of TLC1 was then quantified in this final immunoprecipitate; while the positive control (Est2-FLAG-myc) showed robust enrichment, we found no enrichment of TLC1 compared to the negative control (Figure 6B). We conclude that, although the possibility of a weak or transient association between Est2 molecules cannot be ruled out, these negative lines of evidence are consistent with the model that the majority of the TLC1-TLC1 *in vivo* association is independent of an active telomerase enzyme complex.

DISCUSSION

Here we have explored the nature of telomerase RNA-RNA associations *in vivo* in *S. cerevisiae*. We report that ~10% of the TLC1 molecules *in vivo* are physically associated with another TLC1 molecule. We refer to this as TLC1-TLC1 association for simplicity, although the data do not formally exclude the possibility of higher oligomerization forms. This TLC1-TLC1 association increases by two-fold specifically in G1 phase of the cell cycle, and takes place via two distinguishable modes.

First, mutating a sequence in the 3' region of TLC1 that is cleaved off during the production of the mature form of TLC1 reduced TLC1-TLC1 association by about half. The TLC1-TLC1 association of both the mature and the immature TLC1 forms were comparably affected by this 3' sequence mutation. This same sequence has previously been implicated in TLC1-TLC1 association *in vitro* and its mutation shown to shorten telomeres (Gipson et al., 2007). Our findings thus indicate this 3' sequence-dependent mode of TLC1-TLC1 association occurs *in vivo* during telomerase biogenesis. This is further consistent with our findings that TLC1-TLC1 association depends on nuclear export to the cytoplasm, where biogenesis of telomerase is reported to occur, and that TLC1-TLC1 association increases in G1 phase, the only time in the cell cycle when TLC1 maturation cleavage is active (Chapon, Cech & Zaug, 1997).

The second mode of TLC1-TLC1 association requires Ku binding to TLC1; mutations preventing Ku-TLC1 interaction reduced TLC1-TLC1 association by about half. The Ku-associated protein Sir4 was also required for this mode. The Sir and Ku complexes are both important factors in maintaining telomeres; their functions include forming silent chromatin at telomeres and recruiting telomeres to nuclear periphery (Boulton & Jackson, 1998; Taddei et al., 2004). Interestingly however, although Sir4 is part of the silent information regulator Sir complex, TLC1-TLC1 association required neither classic silencing (neither Sir2 nor Sir3 was required), nor Ku-mediated telomere tethering to the nuclear periphery (neither Esc1 nor Ctf18 was required).

The additive genetic disruptions of these two modes of *in vivo* TLC1-TLC1 association - RNA sequence mutations in the 3' region of TLC1 and deletion of the protein factors Ku and Sir4 - have an intriguing parallel to the *in vitro* disruptions of TLC1-TLC1 association in the immunoprecipitate, via either competition with excess oligonucleotides (most sensitive in the 3' region) or protease treatment. Each of these two *in vitro* treatments disrupted only a fraction of the TLC1-TLC1 association. Combining these findings, the simplest interpretation is that these two fractions correspond to or overlap with the TLC1 3' sequence-dependent and the Ku/Sir4 dependent association modes respectively.

Simultaneously mutating both the 3' precursor TLC1 sequence and abrogating Ku-TLC1 binding abolished *in vivo* TLC1-TLC1 association to background levels. The epistasis analyses together indicate that for physical TLC1-TLC1 association, Ku and Sir4 act in the same pathway, which is distinct from the pathway requiring the 3' end sequence of the immature TLC1 RNA. Notably, each of the various kinds of mutations that we report here to impair TLC1-TLC1 association also causes telomeres to be shorter than wild-type (Askree et al., 2004), consistent with TLC1-TLC1 association *in vivo* having functional significance.

Our findings indicate two separable and potentially independent modes of TLC1-TLC1 association – the first involving the TLC1 3' region prior to cleavage to the mature form, and a subsequent mode involving Ku/Sir4. We propose a model (Figure 7) by which all TLC1 molecules transiently engage in TLC1-TLC1 association during at least two stages in telomerase

461 biogenesis. The first TLC1-TLC1 association mode occurs prior to TLC1 maturation and
462 requires a sequence in the 3'extension of the TLC1 precursor (Figure 7 Mode 1). It is further
463 stabilized by RNA-RNA or RNA-protein interactions that persist after TLC1
464 cleavage/maturation, which can be partially disrupted *in vitro* by anti-sense oligonucleotides -
465 particularly those complementary to the 3' region of the mature telomerase RNA. Our findings
466 suggest that multiple regions of TLC1 RNA help stabilize the TLC1-TLC1 association, and are
467 consistent with a model of their "unzipping" caused by the addition of competing
468 oligonucleotides.
469
470 The second mode requires Ku complex binding to TLC1 and also depends on Sir4 (Figure 7
471 Mode II). While it is not known when in the biogenesis and maturation of TLC1 Ku (and
472 possibly Ku-bound Sir4) become associated with TLC1, Ku and Sir4 are both thought to
473 function at telomeres, where the vast majority of TLC1 (>95%) is already processed to the
474 mature form (*i.e.* missing the 3' region). Both mature TLC1 and uncleaved precursor TLC1 were
475 found coIP'ed with Est2, albeit with the IP efficiency of the immature form being reduced by
476 about half (data not shown). Thus, cleaving off the 3' region of TLC1 is not an obligatory step
477 for TLC1 in order for it to engage in telomerase enzyme complex formation. This is consistent
478 with the lack of interdependence we found between the 3'sequence-mediated association during
479 TLC1 biogenesis and the Ku/Sir-dependent association.
480
481 The presence of two independent modes and machineries for TLC1-TLC1 association suggest
482 that such interaction reflects an important aspect of yeast telomere maintenance biology; a
483 conclusion reinforced by the telomere shortening that results from all the mutations that
484 disrupted TLC1-TLC1 association. However, this report leaves open the detailed mechanisms of
485 these novel in vivo TLC1-TLC1 physical association modes that we have demonstrated in this
486 study. One speculation is that these RNA-RNA associations may be important for the stability of
487 telomerase RNA as it is shuttled among cytoplasmic and nuclear compartments for various
488 maturation steps; a possible model is that TLC1-TLC1 association assists the RNA in acting as
489 its own chaperone. We can further speculate that this might be an important regulatory step for
490 telomerase activity, as the yeast telomerase holoenzyme shows no physical evidence of
491 oligomerization. For example, a dissociation of TLC1-TLC1 association, which likely requires

492 energy, may act as a switch mechanism for forming a fully competent telomerase holoenzyme.
493 Further research will be needed to decipher the mechanistic and functional significance of
494 intermolecular interactions among telomerase components.
495
496 ACKNOWLEDGEMENTS
497 The authors thank Tracy Chow, Beth Cimini, Kyle Jay, Jue Lin, Imke Listerman, and Dana
498 Smith for critical reading of the manuscript and helpful discussion.
499
500 REFERENCES
501 Alves D, Li H, Codrington R, Orte A, Ren X, Klenerman D, Balasubramanian S. 2008. Single-
502 molecule analysis of human telomerase monomer. *Nat Chem Biol* 4:287–289.
503 Askree SH, Yehuda T, Smolikov S, Gurevich R, Hawk J, Coker C, Krauskopf A, Kupiec M,
504 McEachern MJ. 2004. A genome-wide screen for Saccharomyces cerevisiae deletion
505 mutants that affect telomere length. *Proceedings of the National Academy of Sciences of*
506 *the United States of America* 101:8658–8663.
507 Beattie TL, Zhou W, Robinson MO, Harrington L. 2001. Functional Multimerization of the
508 Human Telomerase Reverse Transcriptase. *Mol. Cell. Biol.* 21:6151–6160.
509 Boulton SJ, Jackson SP. 1998. Components of the Ku-dependent non-homologous end-joining
510 pathway are involved in telomeric length maintenance and telomeric silencing. *The*
511 *EMBO Journal* 17:1819–1828.
512 Bryan TM, Goodrich KJ, Cech TR. 2003. Tetrahymena Telomerase Is Active as a Monomer.
513 *Molecular Biology of the Cell* 14:4794–4804.
514 Chan A, Boulé J-B, Zakian VA. 2008. Two Pathways Recruit Telomerase to Saccharomyces
515 cerevisiae Telomeres. *PLoS Genet* 4:e1000236.

516 Chapon C, Cech TR, Zaug AJ. 1997. Polyadenylation of telomerase RNA in budding yeast. *RNA*
517 *(New York, N.Y.)* 3:1337–1351.
518 Evans SK, Lundblad V. 2002. The Est1 Subunit of Saccharomyces cerevisiae Telomerase Makes
519 Multiple Contributions to Telomere Length Maintenance. *Genetics* 162:1101–1115.
520 Fisher TS, Taggart AKP, Zakian VA. 2004. Cell cycle-dependent regulation of yeast telomerase
521 by Ku. *Nat Struct Mol Biol* 11:1198–1205.
522 Franke J, Gehlen J, Ehrenhofer-Murray AE. 2008. Hypermethylation of yeast telomerase RNA
523 by the snRNA and snoRNA methyltransferase Tgs1. *Journal of Cell Science* 121:3553–
524 3560.
525 Gallardo F, Olivier C, Dandjinou AT, Wellinger RJ, Chartrand P. 2008. TLC1 RNA nucleo-
526 cytoplasmic trafficking links telomerase biogenesis to its recruitment to telomeres.
527 *EMBO J* 27:748–757.
528 Gipson CL, Xin Z-T, Danzy SC, Parslow TG, Ly H. 2007. Functional Characterization of Yeast
529 Telomerase RNA Dimerization. *Journal of Biological Chemistry* 282:18857 –18863.
530 Hiraga S, Robertson ED, Donaldson AD. 2006. The Ctf18 RFC-like complex positions yeast
531 telomeres but does not specify their replication time. *EMBO J* 25:1505–1514.
532 Jain D, Cooper JP. 2010. Telomeric strategies: means to an end. *Annual Review of Genetics*
533 44:243–269.
534 Jiang J, Miracco EJ, Hong K, Eckert B, Chan H, Cash DD, Min B, Zhou ZH, Collins K, Feigon
535 J. 2013. The architecture of Tetrahymena telomerase holoenzyme. *Nature* 496:187–192.
536 De Lange T, Lundblad V, Blackburn E. 2006. *Telomeres, Second Edition*. Cold Spring Harbor
537 Laboratory Press.

538 Lin J, Ly H, Hussain A, Abraham M, Pearl S, Tzfati Y, Parslow TG, Blackburn EH. 2004. A
539 universal telomerase RNA core structure includes structured motifs required for binding
540 the telomerase reverse transcriptase protein. *Proceedings of the National Academy of*
541 *Sciences of the United States of America* 101:14713–14718.
542 Lin J, Blackburn EH. 2004. Nucleolar protein PinX1p regulates telomerase by sequestering its
543 protein catalytic subunit in an inactive complex lacking telomerase RNA. *Genes &*
544 *Development* 18:387 –396.
545 Mozdy AD, Cech TR. 2006. Low abundance of telomerase in yeast: Implications for telomerase
546 haploinsufficiency. *RNA* 12:1721 –1737.
547 Mozdy AD, Podell ER, Cech TR. 2008. Multiple Yeast Genes, Including Paf1 Complex Genes,
548 Affect Telomere Length via Telomerase RNA Abundance. *Mol. Cell. Biol.* 28:4152–
549 4161.
550 Osterhage JL, Talley JM, Friedman KL. 2006. Proteasome-dependent degradation of Est1p
551 regulates the cell cycle-restricted assembly of telomerase in Saccharomyces cerevisiae.
552 *Nat Struct Mol Biol* 13:720–728.
553 Prescott J, Blackburn EH. 1997. Functionally interacting telomerase RNAs in the yeast
554 telomerase complex. *Genes & Development* 11:2790 –2800.
555 Sauerwald A, Sandin S, Cristofari G, Scheres SHW, Lingner J, Rhodes D. 2013. Structure of
556 active dimeric human telomerase. *Nature structural & molecular biology* 20:454–460.
557 Seto AG, Livengood AJ, Tzfati Y, Blackburn EH, Cech TR. 2002. A bulged stem tethers Est1p
558 to telomerase RNA in budding yeast. *Genes & Development* 16:2800 –2812.

559 Shcherbakova DM, Sokolov KA, Zvereva MI, Dontsova OA. 2009. Telomerase from yeast
560 Saccharomyces cerevisiae is active in vitro as a monomer. *Biochemistry (Moscow)*
561 74:749–755.
562 Stellwagen AE, Haimberger ZW, Veatch JR, Gottschling DE. 2003. Ku interacts with telomerase
563 RNA to promote telomere addition at native and broken chromosome ends. *Genes &*
564 *Development* 17:2384 –2395.
565 Taddei A, Hediger F, Neumann FR, Bauer C, Gasser SM. 2004. Separation of silencing from
566 perinuclear anchoring functions in yeast Ku80, Sir4 and Esc1 proteins. *EMBO J*
567 23:1301–1312.
568 Teixeira MT, Forstemann K, Gasser SM, Lingner J. 2002. Intracellular trafficking of yeast
569 telomerase components. *EMBO Reports* 3:652–659.
570 Tsukamoto Y, Kato J, Ikeda H. 1997. Silencing factors participate in DNA repair and
571 recombination in Saccharomyces cerevisiae. *Nature* 388:900–903.
572 Wang L, Dean SR, Shippen DE. 2002. Oligomerization of the telomerase reverse transcriptase
573 from Euplotes crassus. *Nucleic Acids Research* 30:4032–4039.
574 Wenz C, Enenkel B, Amacker M, Kelleher C, Damm K, Lingner J. 2001. Human telomerase
575 contains two cooperating telomerase RNA molecules. *The EMBO Journal* 20:3526–3534.
576 Zappulla DC, Cech TR. 2004. Yeast telomerase RNA: A flexible scaffold for protein subunits.
577 *Proceedings of the National Academy of Sciences of the United States of America*
578 101:10024 –10029.
579

FIGURE LEGENDS

Figure 1 TLC1-TLC1 features and association

1A. Schematic and linear maps of relevant features of TLC1 RNA coding sequence before it is polyadenylated and cleaved (+1-1301). TmG: 5' trimethylG cap (Franke et al. 2008); The binding sites for Ku (+288-335), Est1 (+660-664), and Sm (+1153-1160) proteins are indicated. Telomeric template: (+468-484); CS3 (+719-784) and CS4 (+785-853): two sequences, conserved in budding yeasts, that form two sides of a stem of the evolutionarily conserved telomerase RNA pseudoknot structure (Lin et al. 2004); MS2: site of the tandem inserted MS2 coat protein-binding hairpins used in this work, at BclI site (+1033); cleavage site: the 3' end of the mature TLC1 (+1167); CGCGCG: sequence (+1204) previously implicated in TLC1 *in vitro* dimerization, located in the cleaved-off 3' extension of pre-processed immature TLC1 RNA (Chapon et al. 1997).

1B. Anti-sense oligonucleotides targeted against the full length of TLC1. Each of the 72 anti-sense oligonucleotides are 30 bases in length and overlap with each other by 2-5 bases. The oligos are divided into 9 groups (alternating set of blue and red) of 8 oligos.

1C. Distinct primer sets were used to distinguish MS2-tagged and untagged TLC1 during qPCR analysis following coIP. MS2-specific primers anneal within the MS2 insert and therefore can only amplify the tagged version of TLC1. The forward primer for the untagged-specific amplification spans the insertion site for the MS2 tag and therefore cannot amplify the tagged version.

1D. MS2/TLC1 level

The amount of untagged and MS2-tagged TLC1 in total RNA normalized to PGK1 mRNA level is shown. TLC1 was expressed from the genomic locus or on a CEN-ARS plasmid. In "Mix" samples, two strains expressing tagged and untagged TLC1 independently were mixed before the lysis step.

1E.

The MS2-tagged TLC1 associated with Est2.

1F. Southern blot comparing telomere lengths in MS2-tagged TLC1 and WT strains (two independent isolates

1G. Detection of TLC1-TLC1 association by co-immunoprecipitation strategy.
The amount of untagged TLC1 co-immunoprecipitated with MS2-tagged TLC1 was used to estimate the fraction of total TLC1 that is dimeric (see Materials and Methods for calculation).

1H.
The immature TLC1 molecules accounts for only 4-8% of the total level of TLC1 molecules. This fraction was unchanged in the co-immunoprecipitated versus total TLC1.

Figure 2. Regions of TLC1 involved in TLC1-TLC1association
2A. Anti-sense oligonucleotides can disrupt TLC1-TLC1association
Anti-sense oligonucleotides were designed against TLC1 and added during the washing step of immunoprecipitation. The amount of TLC1 that remained in dimer is shown. All 72 anti-TLC1 primers or 72 random primers were added. The error bars indicate the standard errors among the experiments.

2B.
Different subsets of oligonucleotides were added during the wash step of immunoprecipitation. Each box represents the TLC1 region targeted by the added oligonucleotides. Each ninth and third region contained 8 and 24 oligonucleotides respectively. Shown in each box is the fraction of TLC1 that remained on the beads after the wash (standard deviation in parentheses).

2C
The TLC1 3’ region that is cleaved off plays a role in TLC1 dimerization.
The fraction of TLC1 in dimer form is calculated in strains that carry mutations that disrupt palindromic sequence in the 3’ region of TLC1. WT=CGCGCG, 42G=CGGGGG, 42C=CCCCCG, 42GC=CGGGGG+CCCCCG. The ratios of the amount of 3’ region to the total

TLC1 were measured in the total RNA and immunoprecipitated RNA. The values were normalized to the average of all values. The error bars indicate the standard errors among the samples.

Figure 3

3A

TLC1 transport to the cytoplasm is required for TLC1-TLC1 association

Shown are TLC1 dimer levels in the deletion mutant strains indicated.The fraction of TLC1 in the dimer form is calculated from the coIP assays and normalized to the average of the wild-type samples in each experiment. Indicated genes involved in TLC1 biogenesis pathway were deleted. The error bars represent standard errors among the samples.

3B

Cells were arrested in alpha-factor, released and collected every 15 minutes. The first sample (t=0 min) is from alpha-factor arrested cells. Levels of cyclin mRNAs measured to track cell-cycle progress. The values are normalized so that the lowest value is 0 and the highest value is 1. The horizontal bars show cell cycle phase ascertained from the measured cyclin mRNA expression levels shown.

3C Total TLC1 levels, tagged and untagged.

3D The fraction of TLC1 in dimer form calculated from coIP experiments. In 3C and D, the values are normalized to the asynchronous sample and the error bars represent the standard deviation between two experiments.

Figure 4. Protein requirements for TLC1-TLC1 association

4A

TLC1 dimerization is partially sensitive to trypsin treatment.

The fraction of TLC1 that remained in the dimer form was measured. The values were normalized to the average of trypsin-treated samples. The error bars represent the standard

deviation between samples. The one-sample t-test value for the comparison with the wild-type is indicated.

4B

TLC1 dimerization is only modestly affected by absence of Est 1, 2 or 3.

4C Est2 interactions with TLC1.

The RNA pseudoknot structure critical for Est2 binding to TLC1 was mutated (tlc1-20 = cs3 and tlc1-21 = cs4) and compensatory mutation (tlc1-22 = cs3-cs4) was introduced. The fraction of TLC1 in the dimer form was calculated from the coIP assay. The values are normalized to the average of the wild-type samples in each experiment. The error bars indicate the standard error between two experiments.

4D TLC1 dimerization requires Ku.

Fraction of TLC1 in the dimer form was calculated from the coIP assay in strains deleted from indicated genes. The values are normalized to the average of the wild-type samples in each experiment. The error bars indicate the standard error among the samples, except for *ctr9Δ* sample, which was done only once.

4E Total TLC1 levels do not determine the fraction of TLC1 in the dimer form.

TLC1 levels, both tagged and untagged, in the total RNA were measured in strains deleted for the indicated genes. The levels were normalized to PGK1 mRNA levels first and then to the wild-type levels.

Figure 5. Two separate pathways of TLC1-TLC1 association

5A. Ku complex binding to TLC1 and Sir4 are required for TLC1-TLC1 association but telomere tethering to the nuclear periphery and telomere silencing are not. Mutations defective in either telomere tethering to nuclear periphery (ctf18 and esc1) or telomere silencing (sir2, sir3 and sir4) are indicated. Fraction of TLC1 in the dimer form are shown, calculated from the coIP assay in mutant strains as indicated.

5B. Lysate was either untreated, mock-treated, or treated with DNase prior to immunoprecipitation. Figure 5C shows the efficient loss of DNA only in DNA treated samples. Despite the loss of DNA in the samples, the TLC1-TLC1 coIP efficiency was not reduced (5B). In "Mix" samples, two strains expressing tagged and untagged TLC1 independently were mixed before the lysis step.

5C. The Ku mutations were combined with *SIR4* deletion. The values are normalized to the average of the wild-type samples in each experiment. The error bars indicate the standard deviation among the samples.

5D. The Ku and Sir4 combined with the mutation in the 3' region.
Fraction of TLC1 in the dimer form was calculated from the coIP assay in mutant strains as indicated. The values are normalized to the average of the wild-type samples in each experiment. The error bars indicate the standard error among the samples.

Figure 6. Lack of Evidence for Est2-Est2 association *in vivo*
6A. The amount of TLC1 immunoprecipitated after sequential immunoprecipitation, anti-FLAG then anti-MYC, was measured. Amount of TLC1 remained in the MYC IP is represented as the fraction of TLC1 immunoprecipitated in the FLAG IP. The table below indicates EST2 fusions with specified tags present in each IP.

6B. Est2 were fused to Myc or HA and were coexpressed. In one strain (right), the CP region was deleted in the Myc-tagged Est2 copy. Lack of TLC1 binding domain in Est2-ΔCP-Myc cannot be compensated by a potential Est2-Est2 interaction between Est2-ΔCP-Myc and Est2-HA.

Figure 7. Two modes of dimerization model
Top: Schematic of TLC1 cleavage of 3' region. Tick marks: template region of TLC1. CGCGCG: sequence at the 3' region important in TLC1 dimerization. The stem-loop structure that the Ku complex binds is indicated. Middle: Two modes of TLC1-TLC1 association *in vivo*.

156 Mode I, dependent on the precursor TLC1 3’ region, is initiated before the 3’ region is cleaved
157 off (note that base-pairing between the palindromic sequences is not suggested here). Mode II,
158 dependent on Sir4 and the Ku complex, possibly at telomeres. Rectangles: chromosomal
159 telomeric DNA repeats. TLC1 in the telomerase RNP is either monomeric or dimeric, but each
160 RNP contains only one Est2 (bottom).
161

Figure 1

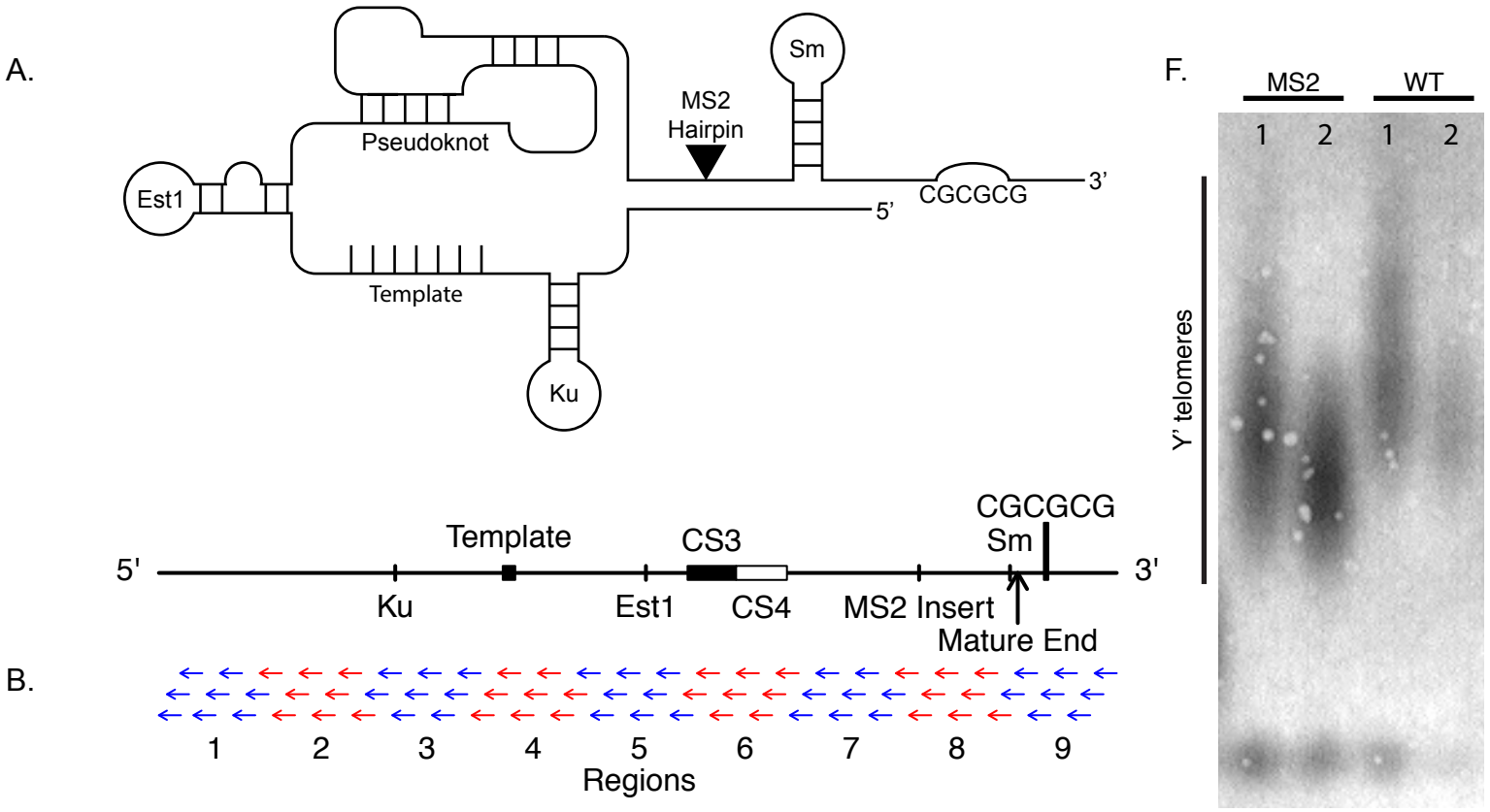
A.
Sm
MS2
Hairpin
Pseudoknot
Est1
CGCGCG
3'
5'
Template
Ku
CGCGCG
Sm
Template
CS3
5'
3'
Ku
Est1
CS4
MS2 Insert
Mature End
B.
1
2
3
4
5
6
7
8
9
Regions
C.
MS2 Insert
MS2
Specific
TLC1
Untagged
Specific
F.
MS2
WT
1
2
1
2
Y' telomeres

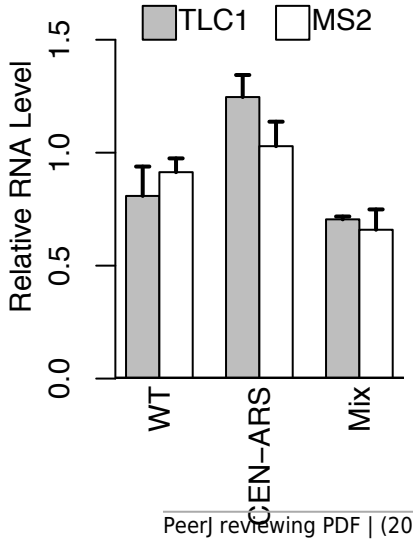
D.
TLC1
MS2
Relative RNA Level
0.0
0.5
1.0
1.5
WT
CEN-ARS
Mix

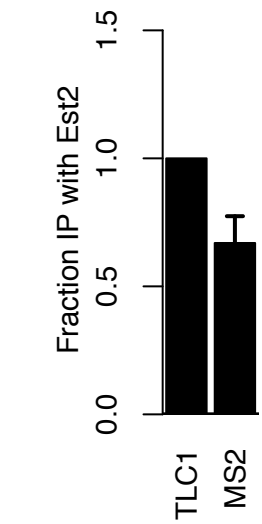
E.
Fraction IP with Est2
0.0
0.5
1.0
1.5
TLC1
MS2

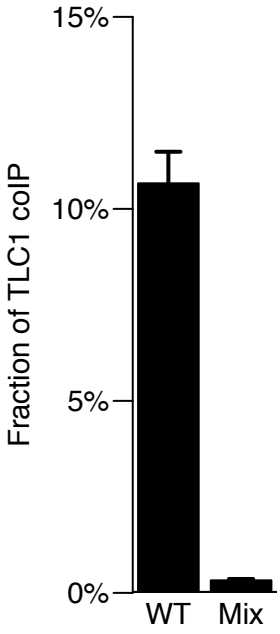
G.
Fraction of TLC1 coIP
15%
10%
5%
0%
WT
Mix

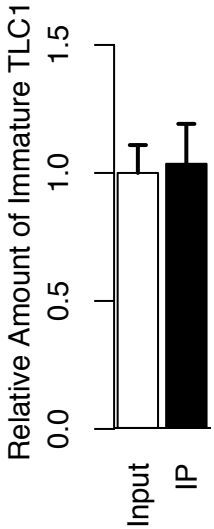
H.
Relative Amount of Immature TLC1
0.0
0.5
1.0
1.5
Input
IP

Figure 2

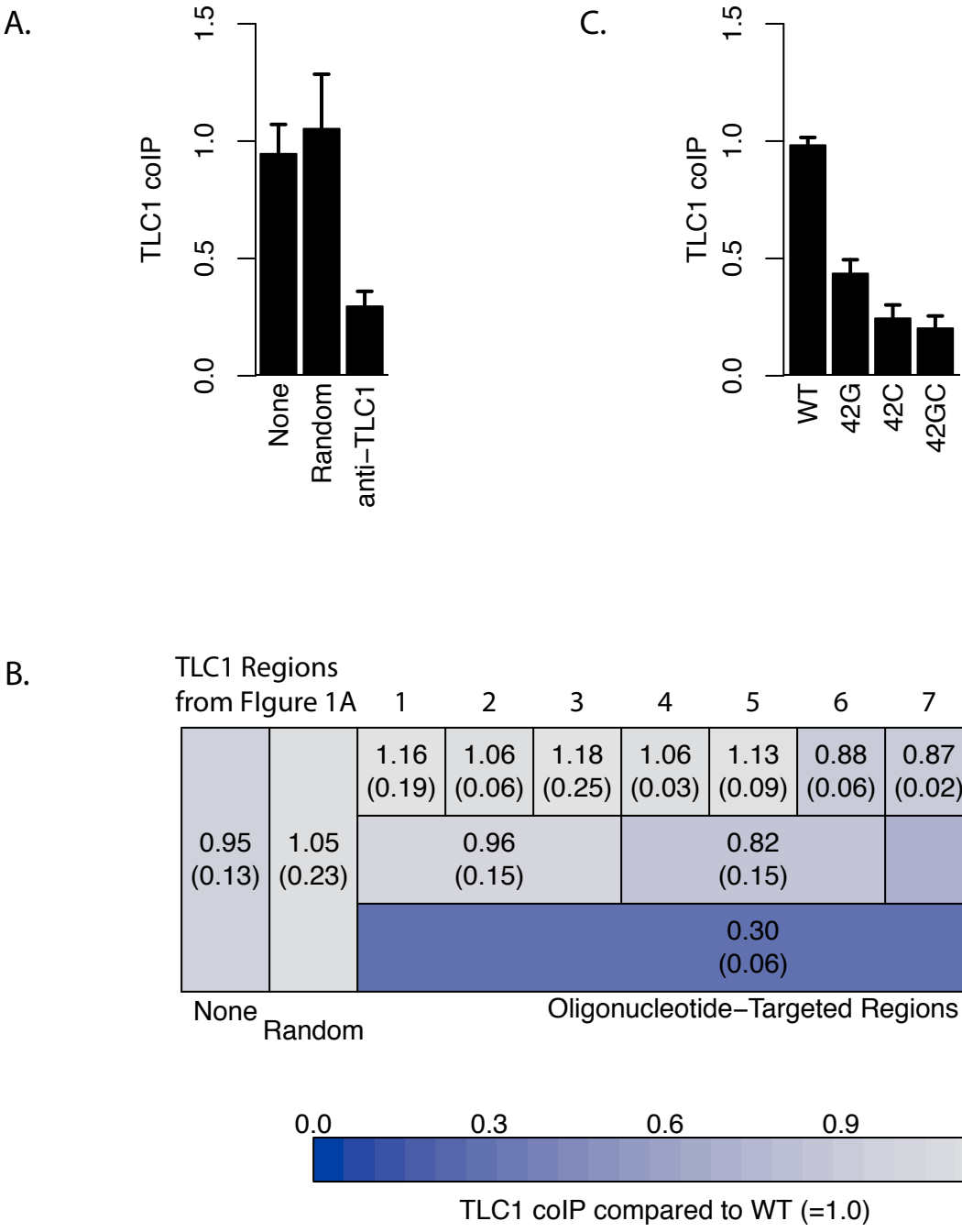
A.
TLC1 coIP
0.0
0.5
1.0
1.5
None
Random
anti–TLC1
C.
TLC1 coIP
0.0
0.5
1.0
1.5
WT
42G
42C
42GC
B.
TLC1 Regions
from FIgure 1A
1
2
3
4
5
6
7
8
9
1.16 (0.19)
1.06 (0.06)
1.18 (0.25)
1.06 (0.03)
1.13 (0.09)
0.88 (0.06)
0.87 (0.02)
0.99 (0.14)
0.70 (0.05)
0.95 (0.13)
1.05 (0.23)
0.96 (0.15)
0.82 (0.15)
0.66 (0.03)
0.30 (0.06)
None
Random
Oligonucleotide–Targeted Regions
0.0
0.3
0.6
0.9
1.2
TLC1 coIP compared to WT (=1.0)

Figure 3

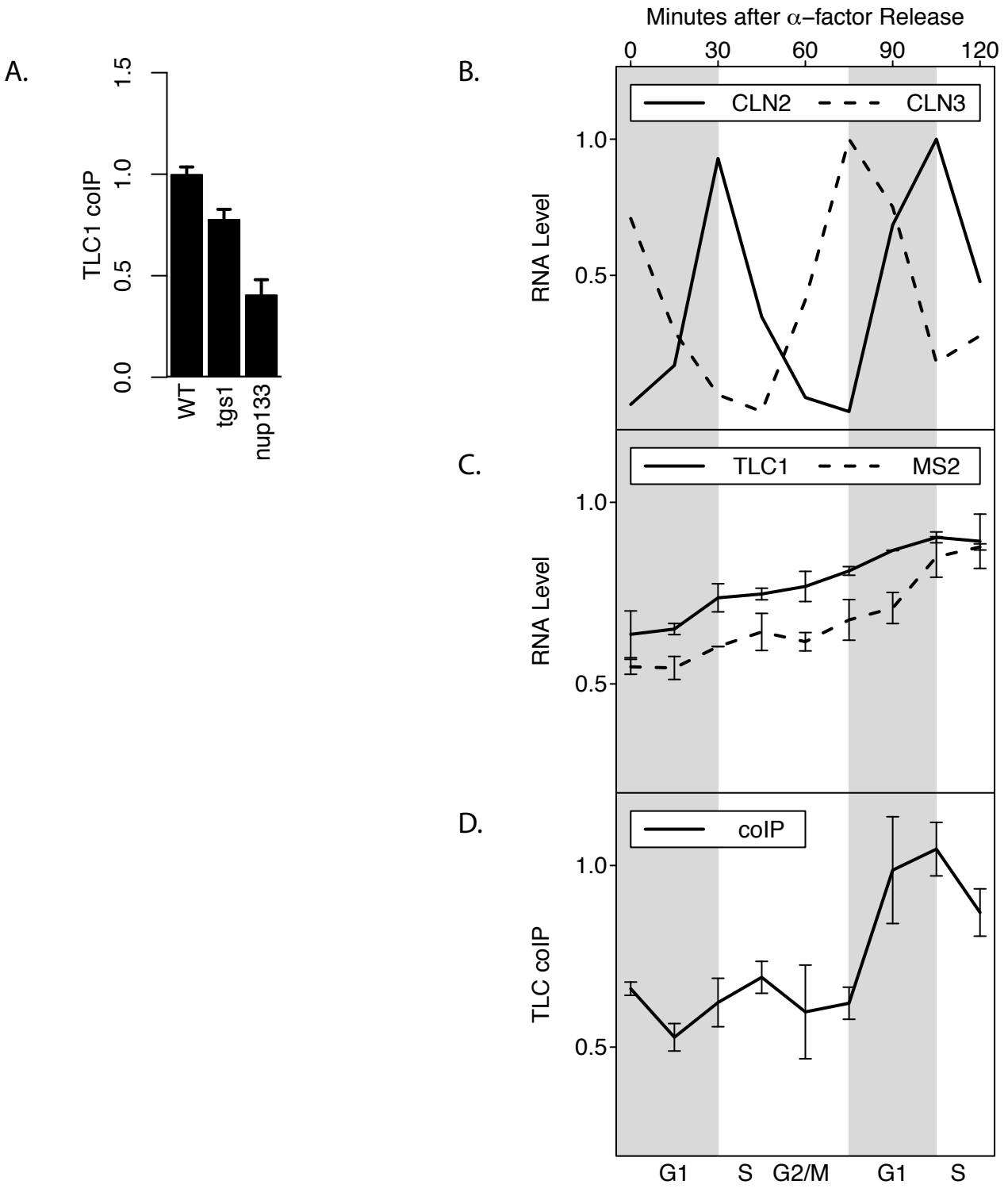
A.
TLC1 coIP
0.0
0.5
1.0
1.5
WT
tgs1
nup133
B.
Minutes after α−factor Release
0
30
60
90
120
CLN2
CLN3
RNA Level
1.0
0.5
C.
TLC1
MS2
RNA Level
1.0
0.5
D.
coIP
TLC coIP
1.0
0.5
G1
S
G2/M
G1
S

Figure 4

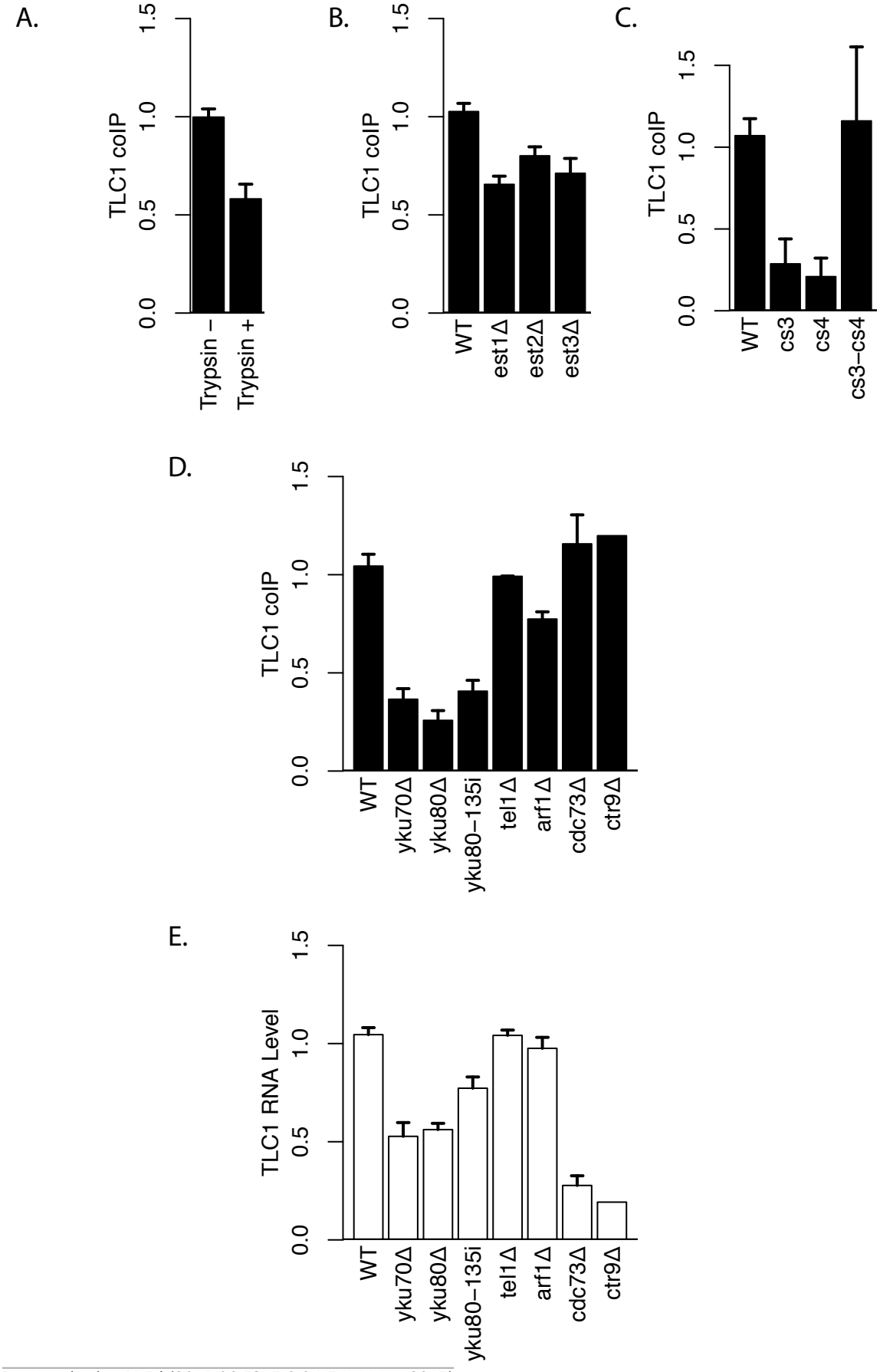
A.
TLC1 coIP
0.0
0.5
1.0
1.5
Trypsin –
Trypsin +
B.
TLC1 coIP
WT
est1Δ
est2Δ
est3Δ
C.
TLC1 coIP
WT
cs3
cs4
cs3–cs4
D.
TLC1 coIP
WT
yku70Δ
yku80Δ
yku80–135i
tel1Δ
arf1Δ
cdc73Δ
ctr9Δ
E.
TLC1 RNA Level
WT
yku70Δ
yku80Δ
yku80–135i
tel1Δ
arf1Δ
cdc73Δ
ctr9Δ

Figure 5

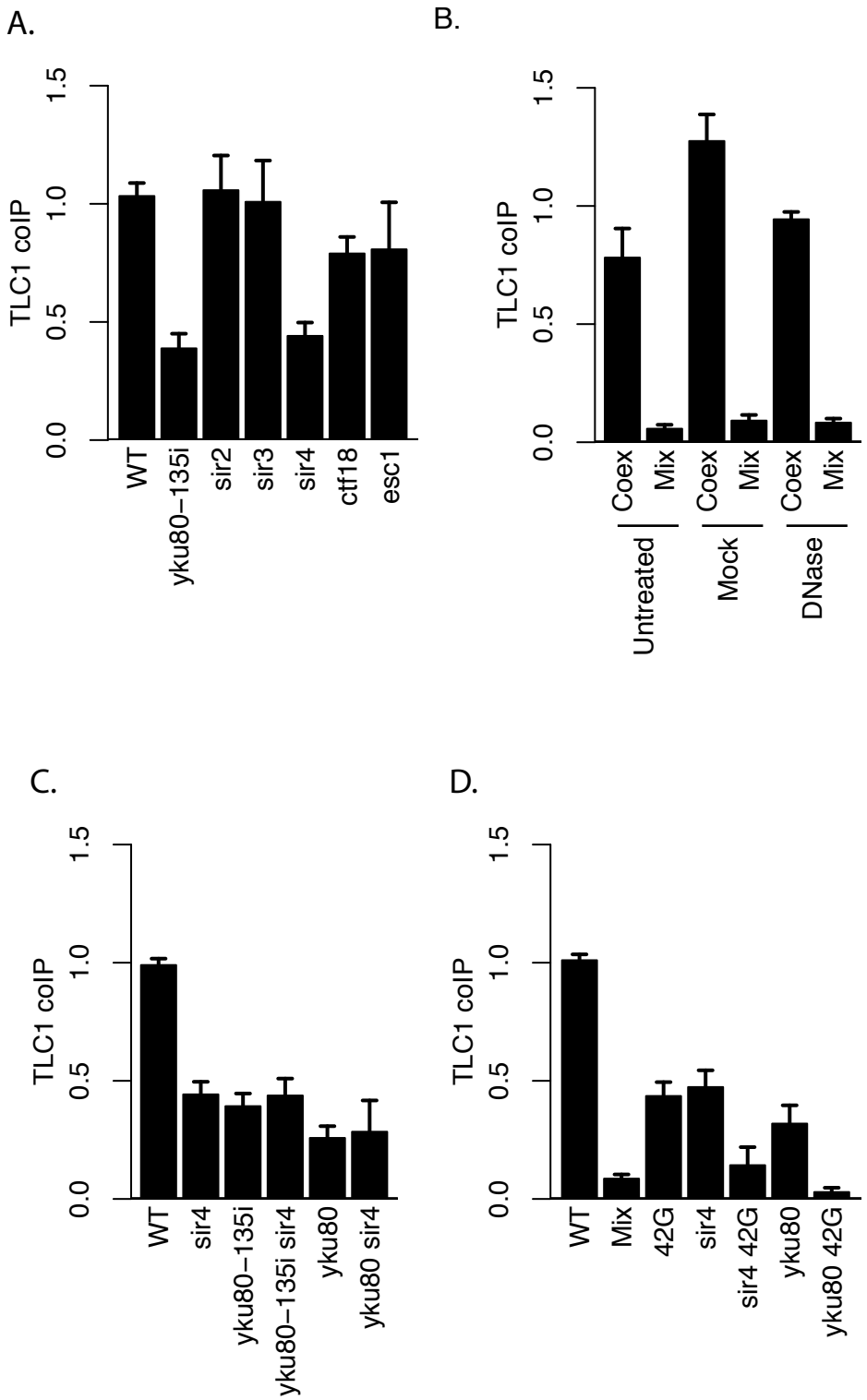
A.
TLC1 coIP
0.0
0.5
1.0
1.5
WT
yku80−135i
sir2
sir3
sir4
ctf18
esc1
B.
TLC1 coIP
0.0
0.5
1.0
1.5
Coex
Mix
Coex
Mix
Coex
Mix
Untreated
Mock
DNase
C.
TLC1 coIP
0.0
0.5
1.0
1.5
WT
sir4
yku80−135i
yku80−135i sir4
yku80
yku80 sir4
D.
TLC1 coIP
0.0
0.5
1.0
1.5
WT
Mix
42G
sir4
sir4 42G
yku80
yku80 42G

Figure 6

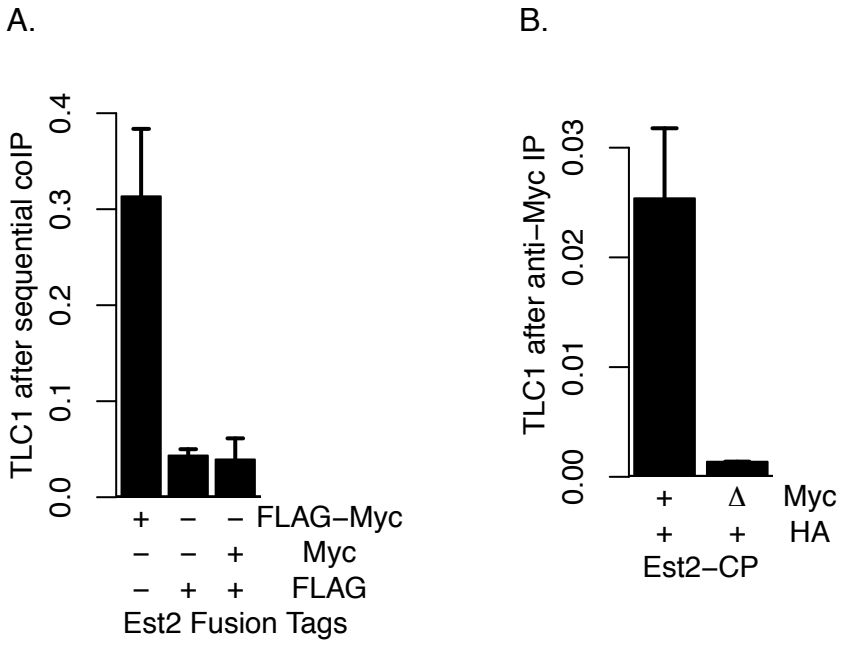
A.
TLC1 after sequential coIP
0.0
0.1
0.2
0.3
0.4
+ − − FLAG−Myc
− − + Myc
− + + FLAG
Est2 Fusion Tags
B.
TLC1 after anti−Myc IP
0.00
0.01
0.02
0.03
+ Δ Myc
+ + HA
Est2−CP

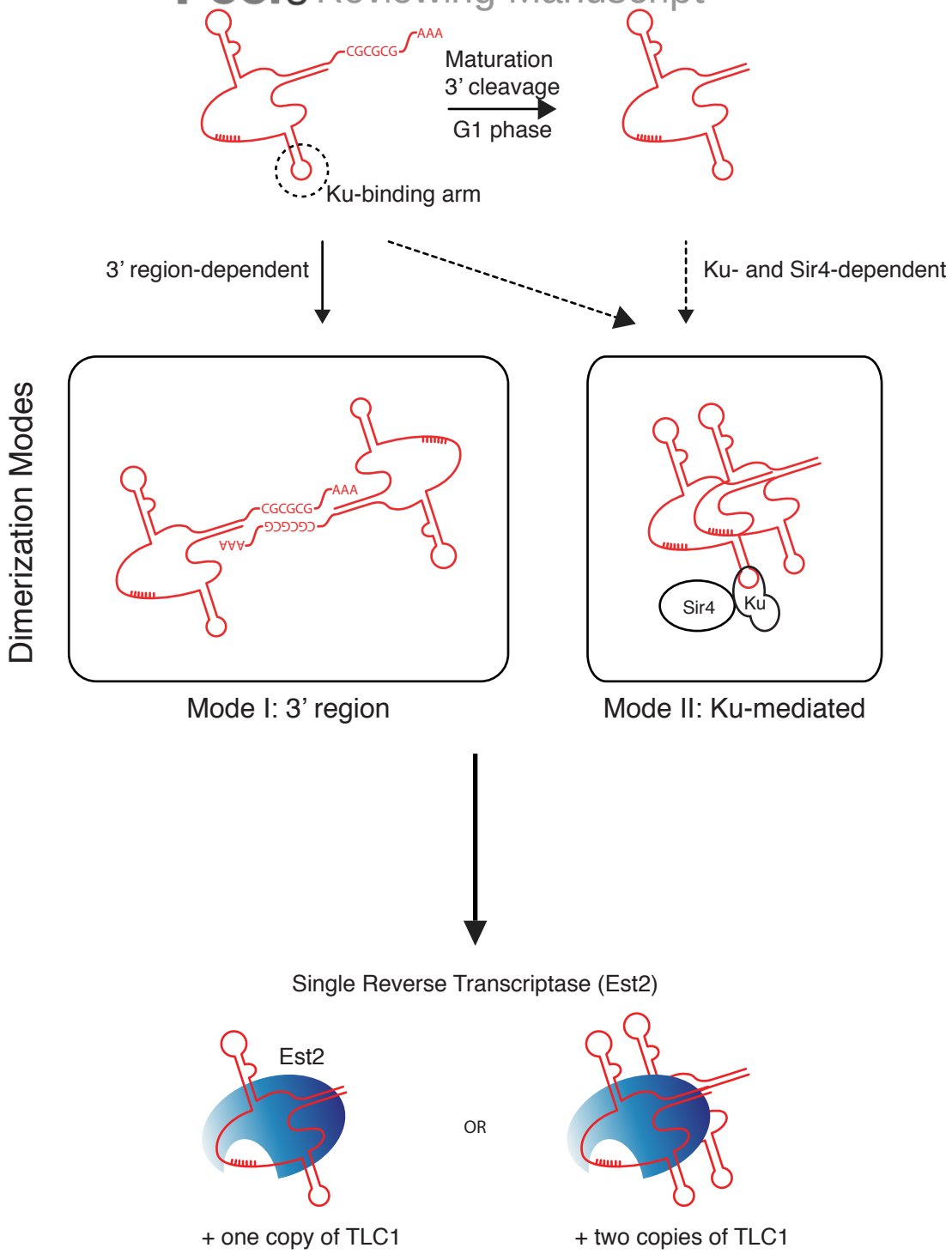

Table 1. Strains used.

All strains are in the S288c strain background and are isogenic, except as noted below.

Strain number	Relevant genotype
yEHB22,321	*ADE2 his3Δ1 leu2Δ0 lys2Δ0 met15Δ0 trp1Δ63 ura3Δ0 bar1Δ0 MATa*
yEHB22,465	*ADE2 his3Δ1 leu2Δ0 lys2Δ0 met15Δ0 trp1Δ63 ura3Δ0 bar1Δ0 MATa*
yEHB22,495	yEHB22,321 but *TLC1-MS2*
yEHB22,496	yEHB22,465 but *TLC1-MS2*
yEHB22,720	yEHB22,321 but *HIS3-P_{CYC1}-CP-3xMyc*
yEHB22,721	yEHB22,465 but *HIS3-P_{CYC1}-CP-3xMyc*
yEHB22,722	yEHB22,720 but *TLC1-MS2*
yEHB22,723	yEHB22,721 but *TLC1-MS2*
yEHB22,662	yEHB22,720 but *TLC1-URA3-TLC1-MS2*
yEHB22,663	yEHB22,721 but *TLC1-URA3-TLC1-MS2*
yEHB22,750	yEHB22,720 but *TLC1-LEU2-TLC1-MS2*
yEHB22,751	yEHB22,721 but *TLC1-LEU2-TLC1-MS2*
yEHB22,799	yEHB22,720 but *TLC1-URA3-TLC1*
yEHB22,800	yEHB22,721 but *TLC1-URA3-TLC1*
yEHB22,801	yEHB22,720 but *TLC1-MS2-URA3-TLC1-MS2*
yEHB22,802	yEHB22,721 but *TLC1-MS2-URA3-TLC1-MS2*
yEHB22,742	yEHB22,720 but *tlc1-42G-URA3-TLC1-MS2*
yEHB22.743	yEHB22,721 but *tlc1-42G-URA3-TLC1-MS2*
yEHB22.744	yEHB22,720 but *tlc1-42C-URA3-TLC1-MS2*
yEHB22.745	yEHB22,721 but *tlc1-42C-URA3-TLC1-MS2*
yEHB22.776	yEHB22,720 but *tlc1-42C-URA3-tlc1-42G-MS2*
yEHB22.777	yEHB22,721 but *tlc1-42C-URA3-tlc1-42G-MS2*
yEHB22,704	yEHB22,662 but *tgs1Δ::KanMX6*
yEHB22,705	yEHB22,663 but *tgs1Δ::KanMX6*
yEHB22,768	yEHB22,750 but *nup133Δ::KanMX6*
yEHB22,769	yEHB22,751 but *nup133Δ::KanMX6*
yEHB22,698	yEHB22,662 but *est1Δ::KanMX6*
yEHB22,699	yEHB22,663 but *est1Δ::KanMX6*
yEHB22,724	yEHB22,662 but *est2Δ::KanMX6*
yEHB22,725	yEHB22,663 but *est2Δ::KanMX6*
yEHB22,700	yEHB22,662 but *est3Δ::KanMX6*
yEHB22,701	yEHB22,663 but *est3Δ::KanMX6*
yEHB22,682	yEHB22,662 but *yku70Δ::KanMX6*
yEHB22,683	yEHB22,663 but *yku70Δ::KanMX6*
yEHB22,686	yEHB22,662 but *yku80Δ::KanMX6*

yEHB22,687	yEHB22,663 but *yku80Δ::KanMX6*
yEHB22,758	yEHB22,750 but *yku80-135i*
yEHB22,759	yEHB22,751 but *yku80-135i*
yEHB22,702	yEHB22,662 but *arf1Δ::KanMX6*
yEHB22,703	yEHB22,663 but *arf1Δ::KanMX6*
yEHB22,706	yEHB22,662 but *cdc73Δ::KanMX6*
yEHB22,707	yEHB22,663 but *cdc73Δ::KanMX6*
yEHB22,726	yEHB22,662 but *ctr9Δ::KanMX6*
yEHB22,727	yEHB22,663 but *ctr9Δ::KanMX6*
yEHB22,764	yEHB22,750 but *ctf18Δ::KanMX6*
yEHB22,765	yEHB22,751 but *ctf18Δ::KanMX6*
yEHB22,766	yEHB22,750 but *esc1Δ::KanMX6*
yEHB22,767	yEHB22,751 but *esc1Δ::KanMX6*
yEHB22,728	yEHB22,662 but *sir2Δ::KanMX6*
yEHB22,729	yEHB22,663 but *sir2Δ::KanMX6*
yEHB22,762	yEHB22,750 but *sir3Δ::KanMX6*
yEHB22,763	yEHB22,751 but *sir3Δ::KanMX6*
yEHB22,730	yEHB22,662 but *sir4Δ::KanMX6*
yEHB22,731	yEHB22,663 but *sir4Δ::KanMX6*
yEHB22,787	yEHB22,662 but *sir4-42::KanMX6*
yEHB22,788	yEHB22,663 but *sir4-42::KanMX6*
yEHB22,789	yEHB22,662 but *rif1Δ::KanMX6*
yEHB22,790	yEHB22,663 but *rif1Δ::KanMX6*
yEHB22,791	yEHB22,662 but *rif2Δ::KanMX6*
yEHB22,792	yEHB22,663 but *rif2Δ::KanMX6*
yEHB22,770	yEHB22,750 but *tel1Δ::KanMX6*
yEHB22,771	yEHB22,751 but *tel1Δ::KanMX6*
yEHB22,774	yEHB22,662 but *sir4Δ::KanMX6 yku80Δ::TRP1*
yEHB22,775	yEHB22,663 but *sir4Δ::KanMX6 yku80Δ::TRP1*
yEHB22,776	yEHB22,720 but *tlc1-42G-URA3-TLC1-MS2 yku80Δ::TRP1*
yEHB22,777	yEHB22,721 but *tlc1-42G-URA3-TLC1-MS2 yku80Δ::TRP1*
yEHB22,803	*LYS2 can1Δ::STE2$_P$-HIS5 lyp1Δ::STE3$_P$-LEU2*
yEHB22,804	*LYS2 can1Δ::STE2$_P$-HIS5 lyp1Δ::STE3$_P$-LEU2*
yEHB22,805	yEHB22,803 but *TLC1-MS2*
yEHB22,806	yEHB22,804 but *TLC1-MS2*
yEHB22,807	yEHB22,803 but *TLC1-URA3-TLC1-MS2*
yEHB22,808	yEHB22,804 but *TLC1-URA3-TLC1-MS2*
yEHB22,809	yEHB22,803 but *tlc1-42G-URA3-TLC1-MS2*
yEHB22,810	yEHB22,804 but *tlc1-42G-URA3-TLC1-MS2*
yEHB22,811	yEHB22,803 but *tlc1-42C-URA3-TLC1-MS2*

yEHB22,812	yEHB22,804 but *tlc1-42C-URA3-TLC1-MS2*
yEHB22,813	yEHB22,803 but *tlc2-42C-URA3-tlc1-42G-MS2*
yEHB22,814	yEHB22,804 but *tlc2-42C-URA3-tlc1-42G-MS2*
yEHB22,815	yEHB22,807 but *yku80-135i*
yEHB22,816	yEHB22,808 but *yku80-135i*
yEHB22,817	yEHB22,807 but *sir4Δ::KanMX6*
yEHB22,818	yEHB22,808 but *sir4Δ::KanMX6*
yEHB22,819	yEHB22,807 but *sir2Δ::KanMX6*
yEHB22,820	yEHB22,808 but *sir2Δ::KanMX6*
yEHB22,821	yEHB22,807 but *sir4Δ::KanMX6 yku80-135i*
yEHB22,822	yEHB22,808 but *sir4Δ::KanMX6 yku80-135i*
yEHB22,823	yEHB22,803 but *tlc1-42G-URA3-TLC1-MS2 yku80-135i*
yEHB22,824	yEHB22,804 but *tlc1-42G-URA3-TLC1-MS2 yku80-135i*
yEHB22,825	*EST2-3xFLAG/EST2-13xMyc MATa/α*
yEHB22,826	*EST2-3xFLAG/EST2 MATa/α*
yEHB22,827	*EST2-3xFLAG-13xMyc/EST2 MATa/α*

Table 2. Primer sequences for qRT-PCR

Amplicon	Primer number	Sequence (5' to 3')
PGK1	oEHB22,0716	GGCTGGTGCTGAAATCGTTCCAAA
	oEHB22,0717*	AGCCAGCTGGAATACCTTCCTTGT
Untagged *TLC1*	oEHB22,0561	CATCGAACGATGTGACAGAGAA
	oEHB22,0801*	GACAAAAATACCGTATTGATCATTAA
MS2-tagged *TLC1*	oEHB22,0563	ATGCCTGCAGGTCGACTCTAGAAA
	oEHB22,0338*	TGCGACAAAAATACCGTATTGATCA
Uncleaved, untagged *TLC1*	oEHB22,1015	TATCTATTAAAACTACTTTGATGATCAGTA
	oEHB22,1038*	AGCGATATACAAGTACAGTACGCGCG
Uncleaved, MS2-tagged *TLC1*	oEHB22,0339	AGCTTGCATGCCTGCAGGTCGACTC
	oEHB22,1038*	AGCGATATACAAGTACAGTACGCGCG
CLN2	oEHB22,712	TTGTTCGAGCTGTCTGTGGTCACT
	oEHB22,713*	AATTTGGCTTGGTCCCGTAACACG
CLN3	oEHB22,837	AAGGCCGCTGTACAACCTGACTAA
	oEHB22,838*	TGAACCGCGAGGAATACTTGTCCA

*Primer used in the reverse transcription step